

Aligned SF/P(LLA-CL)-blended nanofibers encapsulating nerve growth factor for peripheral nerve regeneration

Zhang Kuihua,^{1*} Wang Chunyang,^{2*} Fan Cunyi,² Mo Xiumei³

¹Department of Polymer Materials and Engineering, College of Materials and Textile Engineering, Jiaying University, Zhejiang 314001, China

²Department of Orthopedic Surgery, Shanghai Sixth People's Hospital, JiaoTong University, Shanghai 200233, China

³State Key Laboratory for Modification of Chemical Fibers and Polymer Materials, College of Materials Science and Engineering, Donghua University, Shanghai 201620, China

Received 5 February 2013; revised 16 May 2013; accepted 11 August 2013

Published online 16 September 2013 in Wiley Online Library (wileyonlinelibrary.com). DOI: 10.1002/jbm.a.34922

Abstract: Artificial nerve guidance conduits (NGCs) containing bioactive neurotrophic factors and topographical structure to biomimic native tissues are essential for efficient regeneration of nerve gaps. In this study, aligned SF/P(LLA-CL) nanofibers encapsulating nerve growth factor (NGF), which was stabilized by SF in core, were fabricated via a coaxial electrospinning technique. The controlled release of NGF from the nanofibers was evaluated using enzyme-linked immune sorbent assay (ELISA) and PC12 cell-based bioassay over a 60-day time period. The results demonstrated that NGF presented a sustained release and remained biological activity over 60 days. Nerve guidance conduits (NGCs) were fabricated by reeling the aligned SF/P(LLA-CL) nanofibrous scaffolds encapsulating NGF and then used as a bridge

implanted across a 15-mm defect in the sciatic nerve of rats to promote nerve regeneration. The outcome in terms of regenerated nerve at 12 weeks was evaluated by a combination of electrophysiological assessment, histochemistry, and electron microscopy. All results clarified that the NGF-encapsulated-aligned SF/P(LLA-CL) NGCs promoted peripheral nerve regeneration significantly better than the aligned SF/P(LLA-CL) NGCs, suggesting that the released NGF from nanofibers could effectively promote the regeneration of peripheral nerve. © 2013 Wiley Periodicals, Inc. *J Biomed Mater Res Part A*: 102A: 2680–2691, 2014.

Key Words: electrospinning, aligned nanofibers, nerve growth factor, peripheral nerve regeneration

How to cite this article: Kuihua Z, Chunyang W, Cunyi F, Xiumei M. 2014. Aligned SF/P(LLA-CL)-blended nanofibers encapsulating nerve growth factor for peripheral nerve regeneration. *J Biomed Mater Res Part A* 2014;102A:2680–2691.

INTRODUCTION

Peripheral nerve regeneration and functional recovery after injury remain challenging over long-lesion gaps despite surgical interventions and entubulation of the injured nerve. Autologous nerve graft is the current gold standard for peripheral nerve repair.¹ However, the use of autografts for long-lesion gaps leads to many drawbacks, such as donor site morbidity, shortage of donor nerve, and inadequate functional recovery.^{2–4} Recently, electrospun nanofibrous scaffolds have become a hot topic for their capacity to provide suitable environment for cell attachment, proliferation, and migration, mainly because of their resemblances to the topographic features of natural extracellular matrix (ECMs).^{5–7} Multifarious biodegradable synthetic and/or natural polymers have been electrospun into nanofibrous scaffolds for various kinds of tissue repair and regeneration, such as bone, cartilage, blood vessel, nerve, skin and bladder regeneration.^{8–10} In previous study, to combine the

advantage of both natural polymer (SF) and synthetic polymer (P(LLA-CL)), electrospun SF/P(LLA-CL)-blended nanofibrous scaffolds have been fabricated and demonstrated greater physical properties, biocompatibility and biodegradation in comparison with pure P(LLA-CL) nanofibrous scaffolds.^{11,12} Moreover, the aligned SF/P(LLA-CL) nanofibrous scaffolds nerve guidance conduits (NGCs) could greatly promote peripheral nerve regeneration compared with the aligned P(LLA-CL) nanofibrous scaffolds NGCs.¹³

To further enhance nerve regeneration of long-lesion gaps, NGCs in combination with neurotrophic factors, such as nerve growth factor (NGF), glial cell line derived neurotrophic factor (GDNF) and neurotrophin NT-3, have been implicated as potential therapeutics for peripheral nerve injury.^{14–17} Because neurotrophic factors play vital roles in dominating the survival, migration, proliferation and differentiation of various neural cell types.¹⁸ Therefore, such NGCs drug delivery systems and the sustained release of

*These authors contributed equally to this work.

Correspondence to: F. Cunyi; e-mail: fancunyi888@hotmail.com (or) M. Xiumei; e-mail: med@dhu.edu.cn

Contract grant sponsor: National Natural Science Foundation of China; contract grant numbers: 31070871; 31271035; 81171477

Contract grant sponsor: Innovation Team Open Funds of Jiaying Municipality; contract grant number: MTC2012-005

Contract grant sponsor: Zhejiang Province University Students' Science and Technology Innovation Program (Miao Talent Plan); contract grant number: 2012R417019

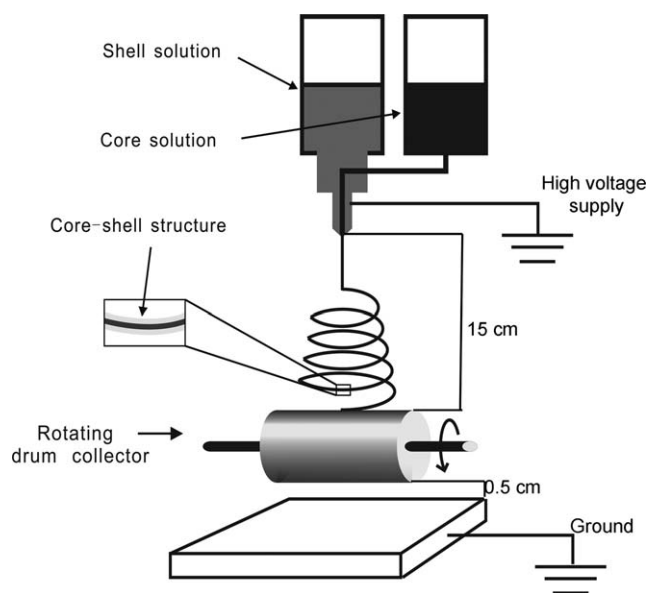


FIGURE 1. Schematic diagram of coaxial electrospinning process.

neurotrophic factors could accelerate axon upgrowth *in vitro* and peripheral nerve regeneration over long gaps *in vivo*.^{19–21} However, ensuring the neurotrophic factors biological activity and sustained release is pivotal due to the instability of such proteins which tend to degrade or aggregate in solution or during processing.^{22,23} Some researchers have investigated the drug delivery systems by mixing drug and polymer into the same solution to fabricate nanofibers. However, the major disadvantage of conventional electrospinning is that the mixed mode often results in burst release of the encapsulated drug. Burst release reduces the effective lifetime of the device and may have toxicological ramifications.²⁴ Therefore, coaxial electrospinning, a simple technique to fabricate continuous composite nanofibers with core-shell structure to load drug has been employed for developing functional scaffolds.²⁵

To further biomimic the natural ECM and control the effective and sustained release of bioactive agents, aligned SF/P(LLA-CL)-blended nanofibers encapsulating NGF were fabricated via coaxial electrospinning method. The influence of SF/P(LLA-CL)-blended nanofibers encapsulating NGF NGCs on nerve regeneration was assessed in a rat sciatic nerve injury model using electrophysiological, histological technique, and electron microscopy.

MATERIALS AND METHODS

Materials

Cocoons of *Bombyx mori* silkworm were kindly supplied by Jiaying Silk Co. (China). A copolymer of P(LLA-CL) (50:50), which has a composition of 50 mol % L-lactide, was provided by Nara Medical University (Japan). 1,1,1,3,3,3-Hexafluoro-2-propanol (HFIP) was purchased from Daikin Industries (Japan). Bovine serum albumin (BSA) was purchased from Sigma-Aldrich. Nerve growth factor (NGF) was purchased from Univ-bio Co. (China). PC12 cells were purchased from ATCC (CRL-1721) (USA). Except specially

explained, all culture media and reagents were purchased from Gibco Life Technologies Co., USA.

Preparation of regenerated SF

Raw silk was degummed three times with 0.5% (w/w) Na_2CO_3 solution at 100°C for 30 min each time and then washed with distilled water. Degummed silk was dissolved in a ternary solvent system of $\text{CaCl}_2/\text{H}_2\text{O}/\text{EtOH}$ solution (1/8/2 in mole ratio) for 1 h at 70°C. The solution was dialyzed with cellulose tubular membrane (250-7u; Sigma) in distilled water for 3 days at room temperature. The distilled water was exchanged every 4 h. The SF solution was filtered and lyophilized to obtain the regenerated SF sponges.

Coaxial electrospinning

BSA was used as the model protein for initial optimization. BSA solution at 5 w/v% in distilled water was prepared for the core solution, SF was added into core solution to increase stability and the concentration was 10–20 w/v%. SF/P(LLA-CL) (weight ratio: 25:75)-blended solution at 8 w/v% in HFIP solvent was prepared for the shell solution.

Figure 1 shows the basic experimental setup for the coaxial electrospinning. The spinneret apparatus consisted of the inner needle (inner diameter: 0.51 mm, outer diameter: 0.80 mm) and the outer one (inner diameter: 1.60 mm). Two syringe pumps (789100C, Cole-Pamer, USA) were used to deliver core and shell solutions through inner and outer needles, respectively. A positive high voltage DC power supply (BGG 6-358, Bmeico, China) was used to generate a maximum 10 kV voltage. To obtain aligned nanobers, a rotating drum collector was used at a speed of 4000 rpm. The distance between the needle and the collector and the oppositely charged metallic plate was 12–15 cm and 18–21 cm, respectively. All processes of electrospinning were operating at room temperature with the relative humidity of 50%. The flow rates of core and shell solutions were set at 0.10–0.20 and 1.0–1.2 mL/h, respectively. The collected nanofibrous scaffolds were placed in vacuum over night to remove the residual solvent.

Characterization of core-shell structured nanofibers

The nanofibrous scaffolds were sputter coated with gold-palladium and observed with a scanning electronic microscope (SEM) (JSM-5600, Japan) at an accelerating voltage of 10 kV. The mean fiber diameters were estimated using an image analysis software (Image-J, National Institutes of Health, USA) and calculated by selecting 100 fibers randomly observed on the SEM images. The 2D fast Fourier transform (FFT) was used to characterize fiber alignment as a function of electrospinning conditions.²⁶ Grayscale 8-bit images were cropped to 2048 × 2048 pixels for analysis. Image J software (NIH, USA) supported by an oval profile plug-in was used to conduct 2D FFT analysis. Pixel intensities were summed along a radius from the center to the edge of the image to quantify the relative contribution of objects oriented in that direction.

Verification of the core-shell structure was conducted by TEM (H-800, Hitachi, Japan) at 100 kV, and the samples

for TEM observations were prepared by collecting the nanofibers onto carbon-coated Cu grids

In vitro release of NGF

Three kinds of aligned electrospun scaffolds encapsulating NGF were fabricated according to above electrospinning parameters. SF/P(LLA-CL)-NGF-blended nanofibrous scaffolds: 100 μ L of 100 μ g/mL of NGF solution was added to 1 mL of 8 w/v% SF/P(LLA-CL) HFIP solution. Core-shell structured SF/P(LLA-CL)-r-NGF nanofibrous scaffolds: 8 w/v% SF/P(LLA-CL) blends in HFIP solvent for the shell solution. A total of 200 μ L of 100 μ g/mL of NGF solution were added to 1 mL sterile ultrapure water. Core-shell structured SF/P(LLA-CL)-r-SF/NGF nanofibrous scaffolds: 8 w/v% SF/P(LLA-CL) blends in HFIP solvent for the shell solution. A total of 200 μ L of 100 μ g/mL of NGF solution was added to 1 mL of 15 wt % SF ultrapure water solution for the core solution. The prepared aligned nanofibrous scaffolds were treated with 75 v/v% ethanol vapor to induce a β -sheet conformational transition of SF, which results in SF insolubility in water.¹³ Three kinds of aligned electrospun scaffolds encapsulating NGF (80 ± 10 mg) were placed in 3 mL of serum-free F12K medium with 1% antibiotic-antimycotic. The test was performed in a 37°C incubator shaker at 50 rpm. At various time points, 1 mL of the supernatant was retrieved from the sealed bottles and replenished with an identical volume of fresh medium. The NGF concentration in the supernatant was then determined by the Duoset ELISA kit (Uni-bio Co. China). Each sample was assayed in triplicate.

Bioactivity of released NGF

PC12 cells, which differentiate to a neuronal phenotype in the presence of bioactive NGF, were used to evaluate the bioactivity of the NGF released from the electrospun nanofibrous scaffolds. PC12 cells were cultured in 24-well plates at a density of 1×10^4 cells/cm². A total of 200 μ L of the NGF supernatant from the nanofibers at days 1, 5, and 60 was added to each well of PC12 cells and F12K medium, supplemented by 2.5% fetal bovine serum, 15% horse serum, and 1% antibiotic and antimycotic formulation, was added to top up to the medium volume to 800 μ L per well. As a positive control, 200 μ L of 1 ng/mL of NGF solution was added to the PC12 cells culture medium, and the total volume of medium was then topped up to 800 μ L with F12K medium. A negative control in which no NGF was added to the F12K medium was also used. Each samples was repeated three times. Images of the PC12 cells were taken 3 days after the supernatant was added into the culture medium.

The fabrication of NGCs and animals experiment

The fabrication process for the NGCs was according to the method described by literature.¹³ The aligned nanofibrous scaffolds were reeled onto a stainless steel bar with a diameter of 1.40 mm and sealed with 8-0 nylon monofilament suture stitches (Shanghai Pudong Jinhuan Medical Products

Co., Shanghai, China), ensuring that the orientation of the nanofibers was parallel to the axis of the bar.

Experiment design and surgical procedures

Thirty-six adult male Sprague-Dawley rats weighing between 220 and 250 g were randomly assigned to one of three experimental groups. Rats in groups I and II were treated by the aligned SF/P(LLA-CL) NGCs and aligned SF/P(LLA-CL)-r-SF/NGF NGCs, respectively. In group III, rats were repaired by autograft. All experimental procedures were carried out in accordance to Institutional Animal Care guidelines and approved ethically by the Administration committee of experimental animals (Shanghai, China).

Rats were anesthetized by intraperitoneal injection of 100 mg/kg ketamine. The right sciatic nerve was exposed and dissected through a dorsal gluteal muscle splitting approach. In groups I and II, a 15 mm nerve segment was excised and removed proximal to the bifurcation of the tibial and peroneal branches, resulting in the creation of a 15 mm nerve gap. Then the gap was bridged by the aligned SF/P(LLA-CL) NGCs (group I) and the aligned SF/P(LLA-CL)-r-SF/NGF NGCs (group II) [Fig. 2(a,b)]. The proximal and distal ends of the nerve stumps were inserted 1 mm into 17-mm long NGCs and sutured to the epineurium by 8-0 nylon sutures [Fig. 2(c)]. In group III, a 15 mm nerve segment was excised, rotated 180° and re-attached to the transected nerve stumps, using 8-0 nylon sutures [Fig. 2(d)].

Electrophysiological evaluation

Six rats in each group were selected for electrophysiological study 12 weeks after implantation. The sciatic nerve was re-exposed under anesthesia, and monopolar recording electrode and bipolar stimulating electrodes were used to induce an electrical activity. The regenerated nerve was stimulated at sites proximal and distal to the NGCs with short duration electrical pulses (Amp 20mA, Freq 1.0s, Dur 0.2 ms), and the evoked compound motor action potential (CMAP) was recorded with electrodes placed on the gastrocnemius muscle. The nerve conduction velocity (NCV) was calculated by dividing the difference of the latencies by the distance between the stimulation points.

Morphological analysis of regenerated nerves

At week 12 postoperatively, the regenerated nerve was exposed and nerve histology was carried out by following procedures. Fixed in situ with 2.5% glutaraldehyde, the regenerated nerve was resected and the middle 3 mm segment was selected for morphological analysis. In groups I and II, the NGCs were removed meticulously before fixation. The middle nerve sections were stored in 2.5% glutaraldehyde in 0.1 mol/L phosphate buffer (pH 7.4) at 4°C. After postfixing with 1% osmium tetroxide and ethanol dehydration, the sections were embedded in EPON 812 (Electron Microscopy Sciences, Hatfield, PA). A total of 1- μ m semithin sections were stained with 1% toluidine blue and observed under light microscopy. A total of 70 nm ultrathin sections were placed on 0.5% formvar-coated meshes and stained

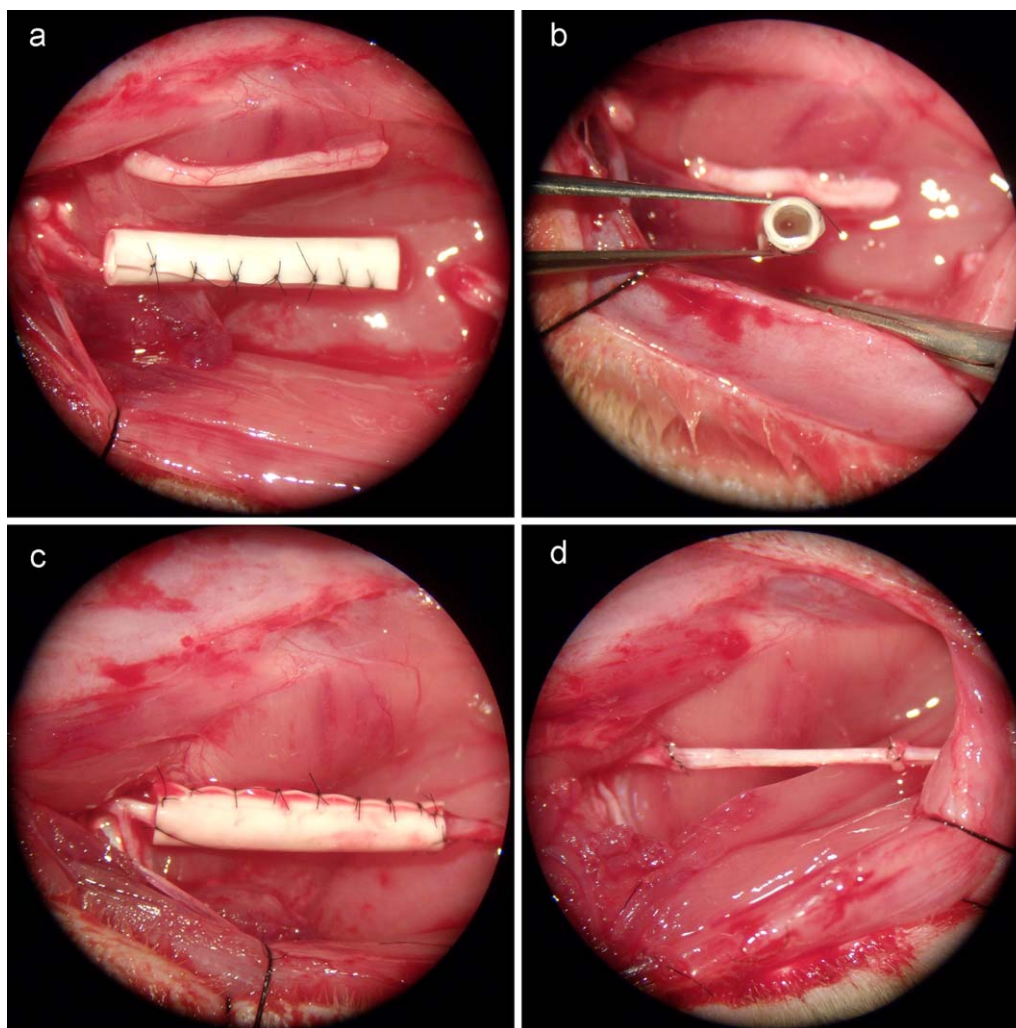


FIGURE 2. Surgical implantation of the aligned NGC for nerve regeneration in a rat sciatic nerve model under a microscope ($\times 10$ magnification). (a, b) The contour of the aligned SF/P(LLA-CL) NGC (group I) and SF/P(LLA-CL)-r-SF/NGF NGC (group II) before implantation; (c) the NGC was used to bridge the 15 mm nerve defect; (d) the autograft never was used to bridge the 15 mm nerve defect. [Color figure can be viewed in the online issue, which is available at wileyonlinelibrary.com.]

with uranyl acetate and lead citrate for TEM study. With the midsections of the regenerated nerve, the number of axons, myelin thickness was quantified for morphological study.

Statistical analysis

The data were expressed as means \pm standard errors of the means. A one-way analysis of variance (ANOVA) was used to compare the autologous control and conduit groups. Followed by Tukey's *post hoc* test using the SPSS 11.0 software package (SPSS, Chicago, IL) for windows student version. The statistical significance of differences between groups was determined as $*p < 0.05$.

RESULTS

Morphology of core-shell structured nanofibers

The SEM morphologies of aligned core-shell structured SF/P(LLA-CL)-r-BSA/SF composite nanofibers were shown in Figure 3. In experimental process, we found that the jet

became unstable and the fluid drop appeared at times when the core solution was 5 w/v% BSA solution without SF.

From Figure 3(a), the mean diameter was 547 ± 198 nm and the alignment of nanofibers was inferior to those with SF in core. Meanwhile, ultrafine-threaded fibers could be found among nanofibers. When adding 10 and 15 w/v% SF into BSA core solution, respectively, the nanofibers became greatly uniform and the average diameters were thicker in comparison with only BSA solutions in core. When the SF increased to 20 w/v% in core BSA solution, the average diameters were thicker than those with 10–15 w/v% SF, and a few nanofibers were bond with together. The 2D FFT analysis of bright field images was used to characterize scaffolds anisotropy and assigned a numerical value to fiber alignment. The degree of fiber alignment was presented by the height and the shape of the peak generated by the 2D FFT plot.²⁷ From Figure 3(i–l), a sharper, higher peak at 90 and 270° than at 0 and 180° indicated the fibers were along a single axis of orientation. For the

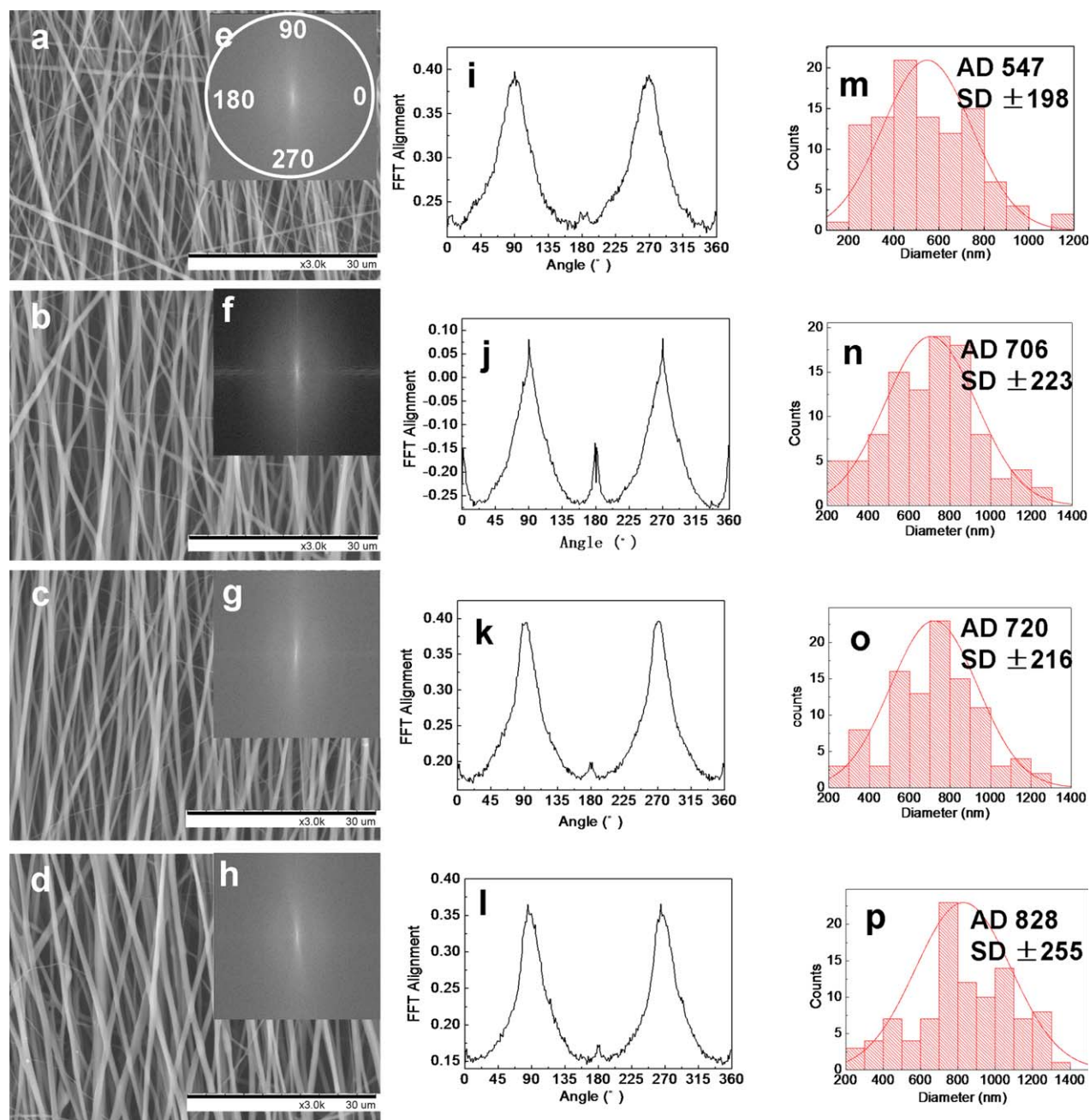


FIGURE 3. SEM micrographs of the aligned core-shell structured nanofibers; 8 w/v% SF/P(LLA-CL) solution as the shell; BSA/SF aqueous solution as the core. (a) 5 w/v% BSA, (b) 5 w/v% BSA+10 w/v% SF, (c) 5 w/v% BSA+15 w/v% SF, (d) 5w/v% BSA+20 w/v% SF, (e–h) corresponding FFT output images and radial projection (e), (i–l) corresponding pixel intensity plots against the angle of acquisition, (m–p) corresponding diameter distribution. [Color figure can be viewed in the online issue, which is available at [wileyonlinelibrary.com](http://www.interscience.wiley.com).]

coaxially aligned electrospun SF/P(LLA-CL)-r-BSA/SF nanofibers, TEM [Fig. 4(a)] micrographs clearly indicated the formation of core-shell structure which had a small fiber embedded in a large fiber. For comparison, Figure 4(b) gives the TEM micrographs of the SF/P(LLA-CL)-blended nanofibers produced using a traditional electrospinning setup.

***In vitro* release of NGF and bioactivity**

To compare the release behavior of different structured nanofibrous scaffolds encapsulating NGF, SF/P(LLA-CL)-

NGF-blended nanofibrous scaffolds, core-shell structured SF/P(LLA-CL)-r-NGF and SF/P(LLA-CL)-r-SF/NGF fibrous scaffolds were fabricated. And NGF release from nanofibers was determined using ELISA. The NGF release profile was shown in Figure 5. Sustained release of NGF from nanofibers was obtained for up to 60 days. NGF in both blended nanofibers and core-shell structured nanofibers have appeared no the initial burst release. NGF was released in a relatively steady manner. NGF was released with near zero-order kinetics. Moreover, NGF was still released until 60

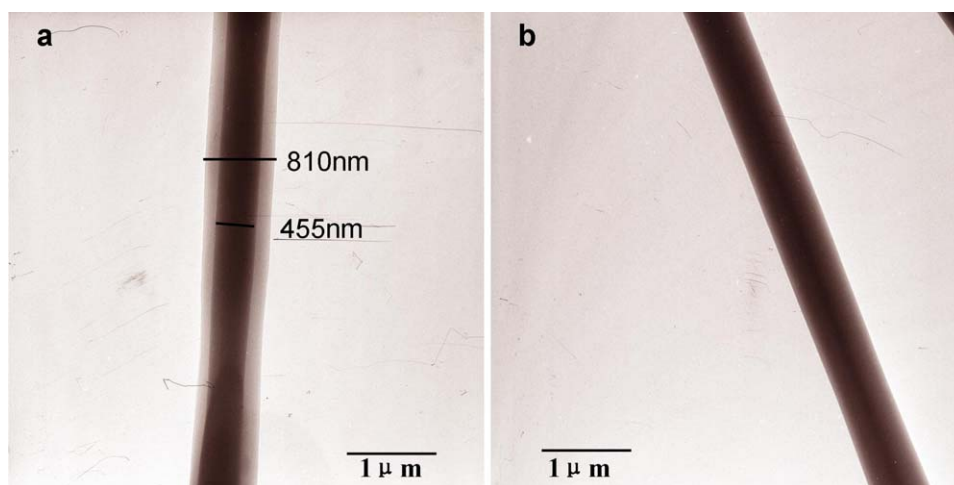


FIGURE 4. TEM micrographs of an individual (a) SF/P(LLA-CL)-r-BSA/SF nanofiber and (b) SF/P(LLA-CL)-blended nanofiber. [Color figure can be viewed in the online issue, which is available at wileyonlinelibrary.com.]

days. After 60 days of released testing, a minor amount of total NGF-amount was released. The cumulative release by day 60 was only 54.76, 46.45, and 39.51 pg/mg, respectively.

The bioactivity of released NGF was evaluated by observing the differentiation of PC12 cells into neurons. The differentiation of the PC12 cells into neurons in the supernatant from the electrospun NGF-encapsulated nanofibers and in the controls was shown in Figure 6. The bioactivity of released NGF was maintained during the entire release testing period of 60 days in different structured nanofibers. However, the amount of neurons was much less than the positive control.

Surgical outcome of implanted NGCs

NGCs were successfully implanted in rats of groups I and II, and no major complications occurred. Twelve weeks after implantation, all animals survived. Exposing the regenerated nerve, the NGCs were surrounded by vascular fascia, and no adhesion with surrounding tissue, as well as no obvious inflammatory, indicating that NGCs had good biocompatibility. And no conduits showed signs of collapse [Fig. 7(a)]. The appearance of regenerated nerve in group II was similar to that in group III [Fig. 7(b-d)].

Electrophysiological evaluation

Both the NCV and CMAP values were objective index of the evaluation of the functional results for the regenerated nerve. The electrophysiology of the regenerated nerve was evaluated by two parameters, NCV and CMAP [Fig. 8(a,b)]. At week 12, the mean NCV calculated was 25.7 ± 2.1 m/s in SF/P(LLA-CL) group, 30.9 ± 4.1 m/s in SF/P(LLA-CL)-r-SF/NGF group and 41.2 ± 1.3 m/s in autograft group. The NCV of regenerated nerve in SF/P(LLA-CL)-r-SF/NGF group was significantly faster than that in negative control group, while slower than that in autograft group [Fig. 8(a)]. The amplitude of CMAP in group II was 6.85 ± 1.36 mV, which was significantly larger than that in group I (5.13 ± 1.12 mV) and was less than that in group III (11.18 ± 1.13 mV) [Fig. 8(b)].

Histological and morphological analysis

The middle samples of the regenerated nerves stained by toluidine blue were used for morphological analysis. Initial qualitative analysis showed that the structure of the regenerated nerve in SF/P(LLA-CL)-r-SF/NGF group was more similar to that in autograft group (Fig. 9) However, the new nerve fibers were much more than those in NGCs groups.

The quantitative analysis of the regenerated nerve was evaluated with parameters of the total axonal area, axon density and total numbers of axon (Fig. 10). Figure 10(a) shows that the area of total axon in NGCs groups was significantly less than that in autograft group ($p < 0.05$), and no statistical difference was observed between NGCs groups ($p > 0.05$). However, the axonal density and the total number of axon in SF/P(LLA-CL)-r-SF/NGF group were significantly more than those in negative control group ($p < 0.05$), though less than those in autograft group [Fig. 10(b,c)].

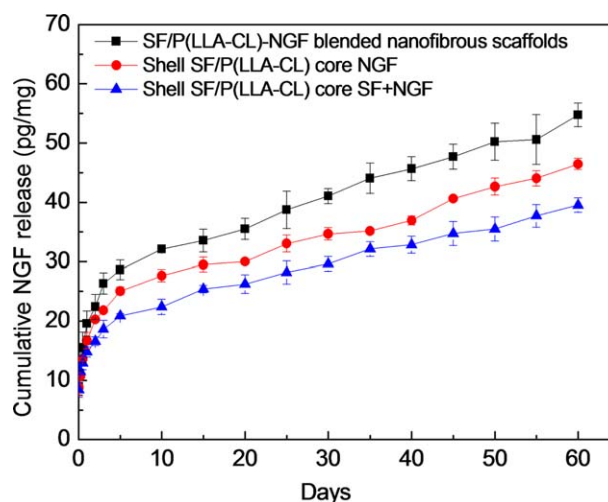


FIGURE 5. Concomitant cumulative release of NGF from different structured aligned nanofibrous scaffolds over 60 days. [Color figure can be viewed in the online issue, which is available at wileyonlinelibrary.com.]

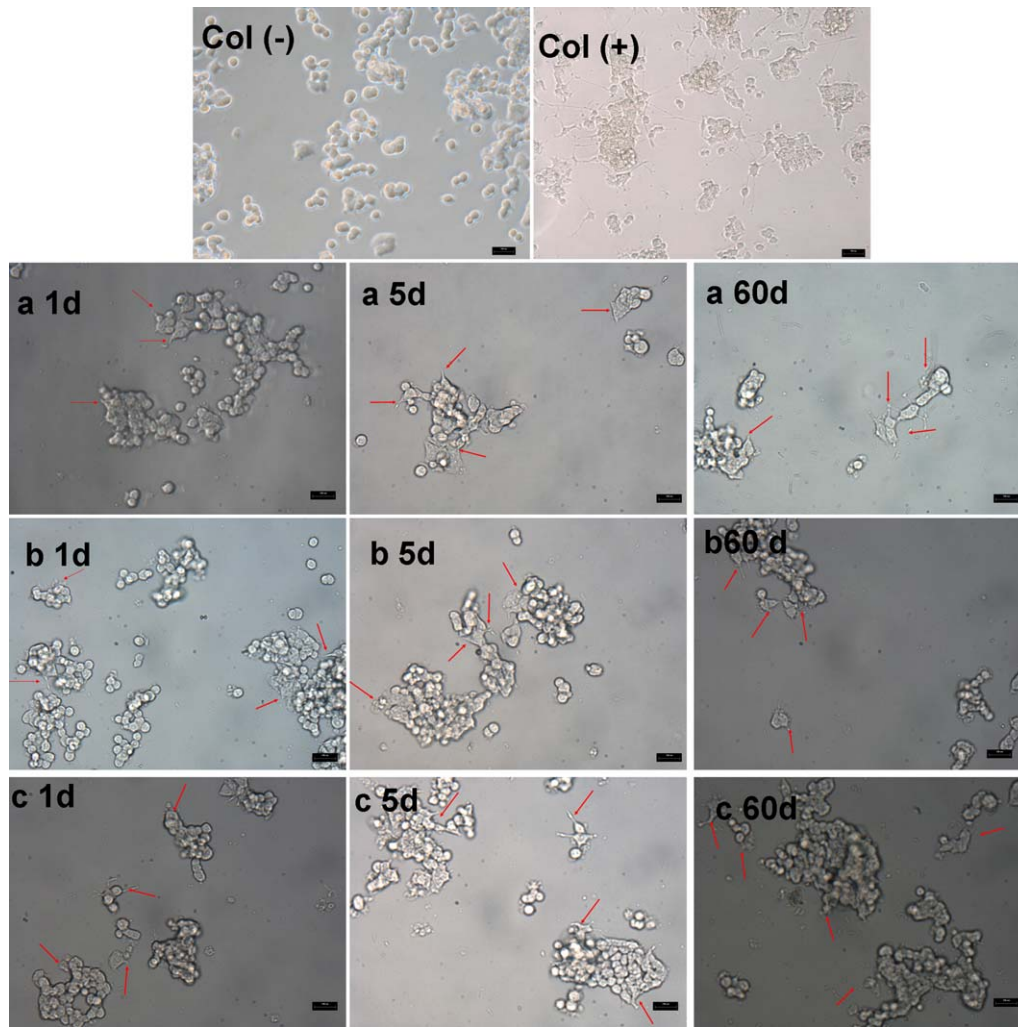


FIGURE 6. Bioactivity of NGF released concomitantly from nanofibers. The bioactivity of NGF was assessed using PC12 cells by addition of released medium collected at days 1, 5, and 60. (a) SF/P(LLA-CL)-NGF-blended nanofibrous scaffolds, (b) SF/P(LLA-CL)-r-NGF nanofibrous scaffolds, (c) SF/P(LLA-CL)-r-SF/NGF nanofibrous scaffolds. For the positive control (Col(+)), 1 ng/mL of NGF was used, whereas negative controls were cultured without NGF(Col(-)). Red arrows mark the neurons of PC12 cells differentiation. [Color figure can be viewed in the online issue, which is available at wileyonlinelibrary.com.]

The ultrastructure of the regenerated nerves was evaluated through electron microscopy. Based on the TEM images, the myelin sheath thickness were compared in each group (Fig. 11). Figure 11(d) shows that the thickness of the myelin was $0.35 \pm 0.08 \mu\text{m}$ in group II, which was thicker than that in group I ($0.27 \pm 0.09 \mu\text{m}$) and thinner than that in group III ($0.62 \pm 0.15 \mu\text{m}$).

DISCUSSION

The wide availability of synthetic NGCs and versatile designs for peripheral nerve regeneration and functional recovery is a major advantage of these conduits over autografts.²⁸ Hence, an increasing number of researchers make effort to the study of synthetic NGCs. The ideal NGCs should biomimic the natural ECMs and provide a more conducive micro-environment for peripheral nerve regeneration.²⁹ Pivotal environment cues for nerve regeneration particularly over

long lesion gaps include appropriate topographic features and molecular factors, such as neurotrophic factors which play an essential role in promoting neuronal survival after injury.¹⁸ The topographical cues presented by aligned electrospun nanofibers could provide better contact guidance towards cells and neurite outgrowth.^{30,31} In this study, we presented the NGF-encapsulated aligned NGCs which was fabricated with core-shell structured SF/P(LLA-CL)-blended nanofibers encapsulating NGF via coaxial electrospinning method. This kind of design not only provided the ideal topographic structure but also controlled sustained release of NGF to significantly improve nerve regeneration.

Silk fibroin (SF) as a natural protein has been widely used in tissue engineering and controlled sustained drug release for its several unique properties including good biocompatibility, good oxygen and water vapor permeability, biodegradability, and commercial availability at a relatively low cost.³²⁻⁴⁰ In this study, SF was selected as the

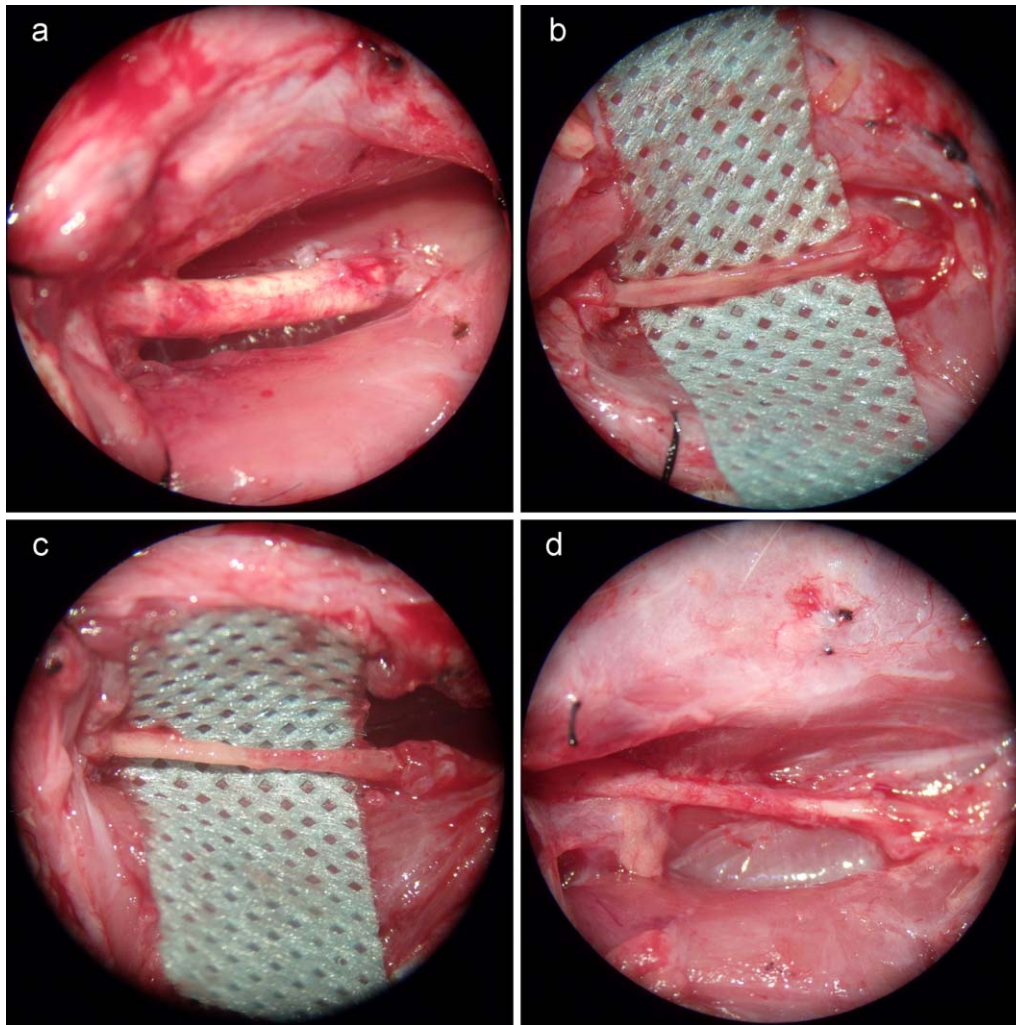


FIGURE 7. Surgical implantation of the NGC for nerve regeneration in a rat sciatic nerve model under a microscope ($\times 10$ magnification). (a) The contour of the NGC 12 weeks after implantation; (b) the regenerated nerve for the aligned SF/P(LLA-CL) NGC (group I); (c) the regenerated nerve for the aligned SF/P(LLA-CL)-r-SF/NGF NGC (group II) 12 weeks after implantation; (d) the autograft nerve (group III) 12 weeks after implantation. [Color figure can be viewed in the online issue, which is available at wileyonlinelibrary.com.]

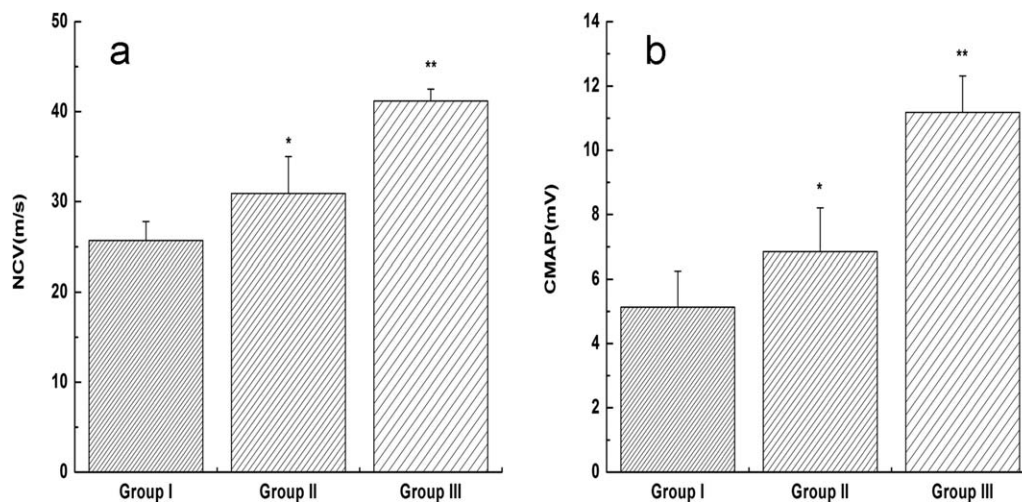


FIGURE 8. Electrophysiological evaluation. (a) NCV evaluation at week 12 after implantation of NGCs (or autograft). (b) CMAP evaluation at week 12 after implantation of NGCs (or autograft). $n = 6$, $*p < 0.05$, determined by LSD analysis of variance (ANOVA).

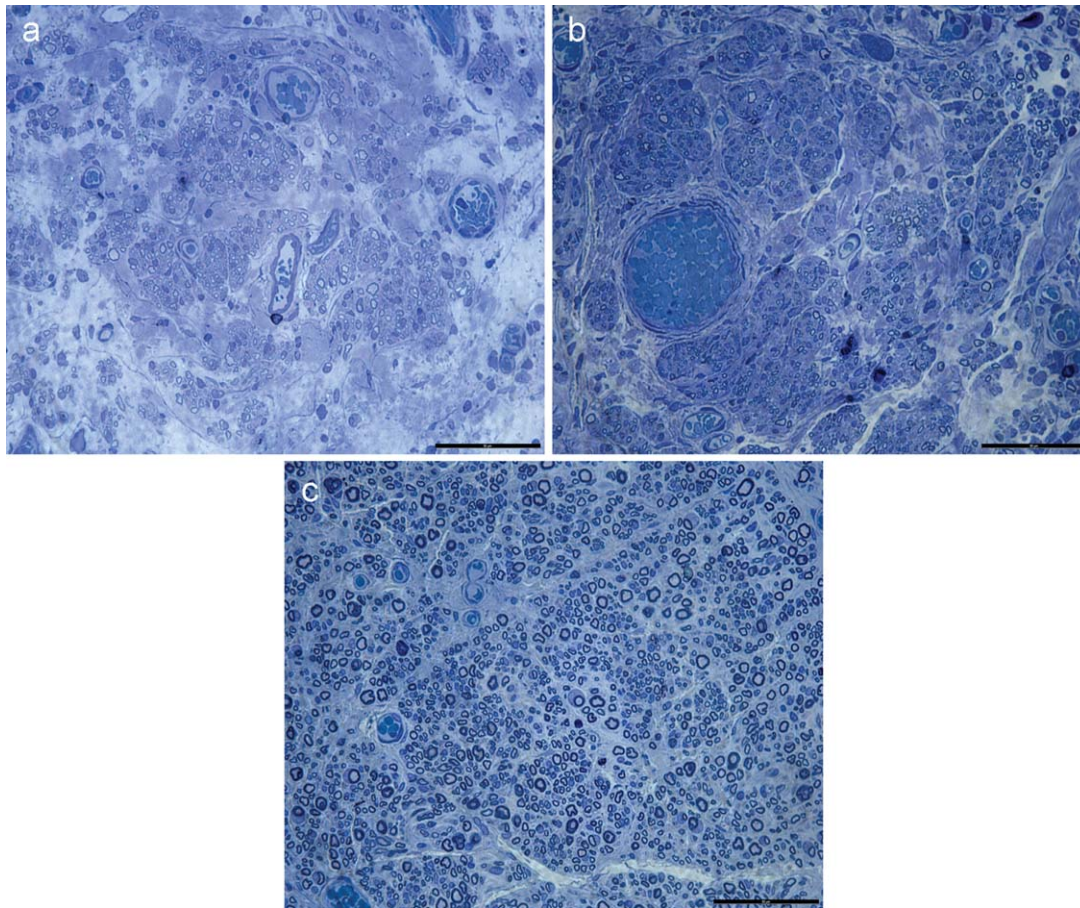


FIGURE 9. Histological sections of regenerated nerves at the middle segment of the conduit (or autograft). Thin (1 μm) sections of regenerated nerve specimens were stained with 1% toluidine blue for qualitative analysis. (a) SF/P(LLA-CL) group; (b) SF/P(LLA-CL)-r-SF/NGF group; (c) autograft group.

stabilizing agent of core solution owing to its spinnability and solubility in water, as well as good combination with NGF.⁴¹ PLLA-CL as shell material provided favorable mechanical properties and biocompatibility for the blended SF/P(LLA-CL) nanofibrous scaffolds.^{11,13} The core-shell structured SF/P(LLA-CL) nanofibers were successfully fabricated using BSA as the model protein. And the addition of 10–15 w/v% SF in core solution enhanced uniformity of nanofibers. It was attributed to the fact that the jet stability of the inner dope increased due to the spinnability of SF polymer. But the further increase of SF in core led to thicker nanofibers and their bond together. Therefore, 15 w/v% SF solution in core was selected to prepare the core-shell structured aligned SF/P(LLA-CL) nanofibers encapsulating NGF using the same electrospinning parameters. Aligned SF/P(LLA-CL)-blended nanofibers loading NGFs were used as a control. The release results of NGF *in vitro* showed that three kinds of nanofibers released NGF at a steady and very low rate over 60 days and presented similar release kinetics. The prolonged release of NGF from nanofibers in the medium at pH about 7.0 was probably attributed to two reasons as follows: (1) there is a strong ionic interaction between the positively charged growth factors (pI 9.3) and

the negatively charged SF (pI 4.3)^{42,43}; (2) the strong H-bond interaction exists between SF molecules and NGF molecules because they are both proteins which have carboxyl groups ($[-\text{COOH}]$) and amino groups ($[-\text{NH}_2]$).

The neuronal differentiation of PC12 cells demonstrated that the biological activity of NGF still remained over 60 days. But the amount of neurons was much inferior to the positive control. A explanation may be that the released NGF per day was too less to induce plenty of neuronal differentiation of PC12 cells. The slow release pattern for NGF should be biologically advantageous, as high amounts of NGF caused extensive branching of regenerating axons resulting in specific target innervation.^{44,45} Moreover, a high burst release would be biologically detrimental and delay the early phase of axonal regeneration by retarding the neuronal perception of reduced levels of endogenous NGF caused by denervation.⁴⁶ Therefore, it was greatly beneficial to long gap nerve repair due to ensuring the provision of NGF under repair process.

Although three kinds of nanofibrous scaffolds loading NGF could carry on slower and controllable release, the aligned SF/P(LLA-CL)-r-SF/NGF nanofibrous scaffolds should be the optimal selection from future clinical application and electrospinning stability points. Because the

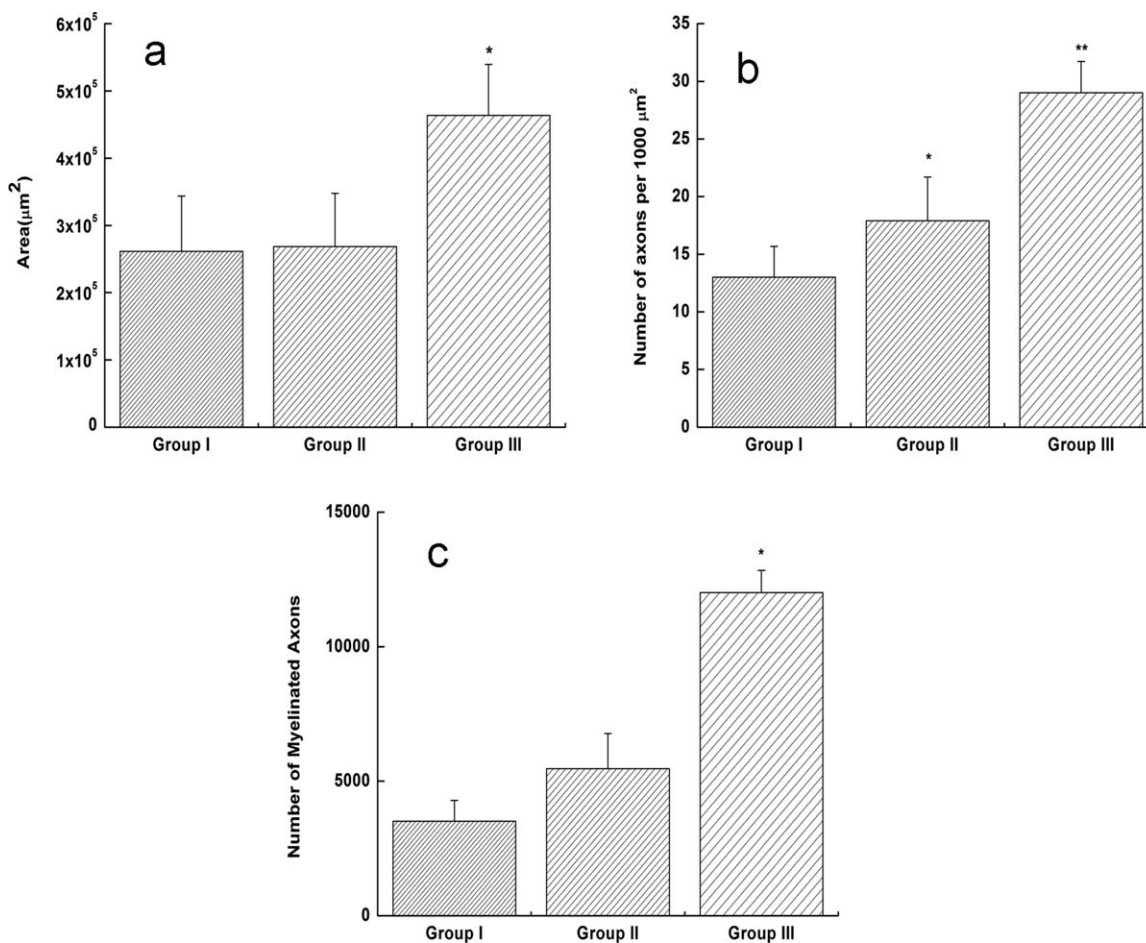


FIGURE 10. Histomorphometric analysis of regenerated nerves at the middle segment of the conduit (or autograft). (a) The area of the regenerated nerve in each group at week 12. (b) The amount of axons in each group at week 12. (c) The amount of myelinated axons in each group at week 12. (d) The thickness of myelin sheath in each group at week 12.

loading efficiency and the bioactivity of NGF were reduced due to the possible aggregation of the protein aqueous droplets suspended in organic solution and the long time exposure of bioactive proteins to organic solvent during blend-electrospinning process.^{47,48} Moreover, the addition of SF in core solution could enhance electrospinning stability (Fig. 3) to make NGF completely loaded in core of nanofibers. Therefore, SF/P(LLA-CL)-r-SF/NGF nanofibrous scaffolds were fabricated as NGCs for the subsequent study on the rat sciatic nerve gap defect. The loaded amount of NGF was increased on the basis of above release results.

In this study, *in vivo*, the conduits to bridge severed sciatic nerves showed hardly any systemic or regional toxic response among the rats in the postoperation period. At 12-week postoperation, the implanted conduits still maintained lumen and wall integrity. This outcome demonstrated that the conduits could provide an excellent microenvironment conducive to axonal regrowth and nerve regeneration until vascularization of the regenerated tissue. The reports of degradation behaviors of SF-NGCs *in vivo* displayed that degradation rate meet the requirement of peripheral nerve regeneration.³⁴ Our findings of SF/P(LLA-CL) nanofibrous scaffolds degradation *in vitro* showed that degradation

properties were superior to pure SF and pure P(LLA-CL) nanofibrous scaffolds.¹² Further study will focus on the biodegradation properties *in vivo*.

The electrophysiological, histological analysis and electron microscopy were used to evaluate the influence of the aligned SF/P(LLA-CL)-r-SF/NGF NGCs on nerve peripheral regeneration. Electrophysiological examination demonstrated significantly better restoration of NCV and CMAP in the SF/P(LLA-CL)-r-SF/NGF NGCs group, indicating that functional recovery of the regenerated nerve was superior to that in the aligned SF/P(LLA-CL) NGCs group. Histological evaluation and electron microscopy indicated that the aligned SF/P(LLA-CL)-r-SF/NGF NGCs group displayed better nerve regeneration in both quantity and quality compared with the aligned SF/P(LLA-CL) NGCs group. All these results showed that loading NGF into aligned SF/P(LLA-CL) nanofibers greatly enhances nerve regeneration. The studies on the enhancement of peripheral nerve regeneration using NGF had demonstrated that NGF might improve sensory and motor nerve regeneration.^{49,50} However, the half-life of NGF is reported to be very short, 1 h,⁵¹ and act at a very low concentration *in vivo*.⁵² Therefore, the sustained release properties of NGF in the aligned SF/P(LLA-CL)-r-SF/NGF

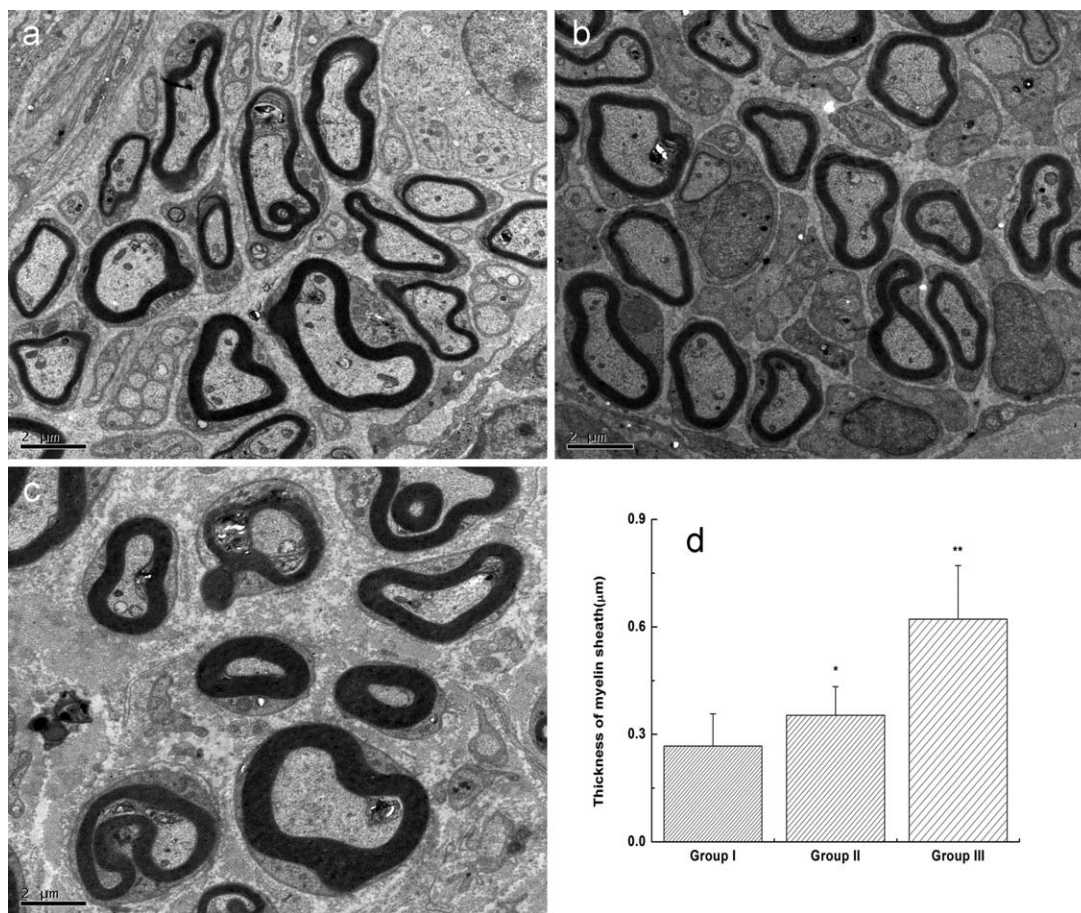


FIGURE 11. Ultrastructure of the regenerated nerve under TEM at week 12 postoperatively. (a) P(LLA-CL) group; (b) SF/P(LLA-CL) group; (c) autograft group; (d) the myelin sheath thickness of each group. $n = 6$, $*p < 0.05$, determined by LSD analysis of variance (ANOVA).

nanofibrous scaffolds were favorable for peripheral nerve regeneration.

In all, the nerve regeneration results of bridging severed sciatic nerves of rats at the 12th week after surgery showed that the aligned SF/P(LLA-CL)-r-SF/NGF NGCs could greatly promote the regeneration of peripheral nerve defect in comparison with SF/P(LLA-CL) NGCs. Combined with the strong mechanical properties and good degradation properties, as well as its favorable biocompatibility of SF and P(LLA-CL), the biodegradable SF/P(LLA-CL)-r-SF/NGF NGCs should be developed into a kind of potential materials to repair nerve damage.

CONCLUSION

In this study, the aligned SF/P(LLA-CL) nanofibers encapsulating NGFs were successfully fabricated via a coaxial electrospinning technique. Nanofibers scaffolds showed sustained release of bioactive NGF over 60 days. The prepared aligned SF/P(LLA-CL) encapsulating NGF NGCs was used as a bridge implanted across a 15-mm defect in the sciatic nerve of rats and the outcome in terms of regenerated nerve at 12 weeks. All results demonstrated that the aligned SF/P(LLA-CL) encapsulating NGF NGCs greatly promoted peripheral nerve regeneration in comparison with the aligned SF/P(LLA-CL) NGCs, suggesting that the NGF of

sustained release from nanofibers was conducive to peripheral nerve regeneration. Thus, NGCs may have a potential application in future peripheral nerve repair.

REFERENCES

- Johnson EO, Zoubos AB, Soucacos PN. Regeneration and repair of peripheral nerves. *Injury* 2005;36:24–29.
- Chen MB, Zhang F, Lineaweaver WC. Luminal fillers in nerve conduits for peripheral nerve repair. *Ann Plast Surg* 2006;57:462–471.
- Bellamkonda RV. Peripheral nerve regeneration: An opinion on channels, scaffolds and anisotropy. *Biomaterials* 2006;27:3515–3518.
- Bini TB, Gao S, Xu X, Wang S, Ramakrishna S, Leong KW. Peripheral nerve regeneration by microbraided poly(L-lactide-co-glycolide) biodegradable polymer fibers. *J Biomed Mater Res A*. 2004; 68:286–295.
- Reneker DH, Chun I. Nanometer diameter fibers of polymer produced by electrospinning. *Nanotechnology* 1996;7:216–223.
- Xu CY, Inai R, Kotaki M, Ramakrishna S. Aligned biodegradable nanofibrous structure: A potential scaffold for blood vessel engineering. *Biomaterials* 2003;25:877–886.
- Ma Z, Kotaki M, Inai R, Ramakrishna S. Potential of nanofiber matrix as tissue-engineering scaffolds. *Tissue Eng* 2005;11:101–109.
- Hong Y, Ye SH, Nieponice A, Soletti L, Vorp DA, Wagner WR. A small diameter, bicuscular conduit generated from a poly(ester urethane) urea and phospholipid polymer blend. *Biomaterials* 2009;30:2457–2467.
- Jha BS, Colello RJ, Bowman JR. Two pole air gap electrospinning: Fabrication of highly aligned, three-dimensional scaffolds for nerve reconstruction. *Acta Biomaterialia* 2011;7:203–215.

10. Cho Y, Choi JS, Jeong SY, Yoo HS. Nerve growth factor (NGF)-conjugated electrospun nanostructures with topographical cues for neuronal differentiation of mesenchymal stem cells. *Acta Biomaterialia* 2010;6:4725–4733.
11. Zhang KH, Wang HS, Huang C, Su Y, Mo XM, Yoshito I. Fabrication of silk fibroin blended P(LLA-CL) nanofibrous scaffolds for tissue engineering. *J Biomed Mater Res: Part A* 2010;93A:984–993.
12. Zhang KH, Yin AL, Huang C, Wang CY, Mo XM, Al-Deyab SS, El-Newehy M. Degradation of electrospun SF/P(LLA-CL) blended nanofibrous scaffolds in vitro. *Polym Degrad Stab* 2011;96:2266–2275.
13. Wang CY, Zhang KH, Fan CY, Mo XM, Ruan HJ, Li FF. Aligned natural-synthetic polyblend nanofibers for peripheral nerve regeneration. *Acta Biomater* 2011;7:634–643.
14. Conti AM, Fischer SJ, Windebank AJ. Inhibition of axonal growth from sensory neurons by excess nerve growth factor. *Ann Neurol* 1997;42:838–846.
15. Sakiyama-Elbert SE, Hubbell JA. Controlled release of nerve growth factor from a heparin-containing fibrin-based cell ingrowth matrix. *J Control Release* 2000;69:149–158.
16. Xu XY, Yu H, Gao SJ, Mao HQ, Leong KW, Wang S. Polyphosphoester microspheres for sustained release of biologically active nerve growth factor. *Biomaterials* 2002;23:3765–3772.
17. Koka LE, Ghaznavi A M, Marra KG. Incorporation of double-walled microspheres into polymer nerve guides for the sustained delivery of glial cell line-derived neurotrophic factor. *Biomaterials* 2010;31:2313–2322.
18. Jiang X, Lim SH, Mao HQ, Chew SY. Current applications and future perspectives of artificial nerve conduits. *Exp Neurol* 2010; 223:86–101.
19. Hari A, Djohar B, Skutella T, Montazeri S. Neurotrophins and extracellular matrix molecules modulate sensory axon outgrowth. *Int J Dev Neurosci* 2004;22:113–117.
20. Xu HX, Yan YH, Li SP. PDLLA/chondroitin sulfate/chitosan/NGF conduits for peripheral nerve regeneration. *Biomaterials* 2011;32: 4506–4516.
21. Fine EG, Decosterd I, Papaliozos M, Zurn AD, Aebischer P. GDNF and NGF released by synthetic guidance channels support sciatic nerve regeneration across a long gap. *Eur J Neurosci* 2002;15: 589–601.
22. Nguyen CB, Szonyi E, Sadick MD, Hotaling TE, Mendoza-Ramirez JL, Escandon E. Stability and interactions of recombinant human nerve growth factor in different biological matrices: In vitro and in vivo studies. *Drug Metab Dispos* 2000;28:590–597.
23. Lam XM, Duenas ET, Cleland JL. Encapsulation and stabilization of nerve growth factor into poly(lactic-co-glycolic) acid microspheres. *J Pharm Sci* 2001;90:1356–1365.
24. Huang X, Brazel CS. On the importance and mechanisms of burst release in matrix-controlled drug delivery systems. *J Control Release* 2001;73:121–136.
25. Zhang YZ, Venugopal J, Huang ZM, Lim CT, Ramakrishna S. Characterization of the surface biocompatibility of the electrospun PCL-collagen nanofibers using fibroblasts. *Biomacromolecules* 2005;6:2583–2589.
26. Ayres CE, Shekhar Jha B, Meredith H, Bowman JR, Bowlin GL, Henderson SC, Simpson DG. Measuring fiber alignment in electrospun scaffolds: A user's guide to the 2D fast Fourier transform approach. *J Biomater Sci: Polym Ed* 2008;19:603–621.
27. Ayres C, Bowlin GL, Henderson SC, Taylor L, Shultz J, Alexander J, Telemeco TA, Simpson DG. Modulation of anisotropy in electrospun tissue-engineering scaffolds: Analysis of fiber alignment by the fast Fourier transform. *Biomaterials* 2006;27:5524–5534.
28. Ichihara S, Inada YJ, Nakamura T. Artificial nerve tubes and their application for repair of peripheral nerve injury: An update of current concepts. *Int J Care Injure* 2008;39S4:S29–S39.
29. Madduri S, Papalo M, Gander B. Tropically and topographically functionalized silk fibroin nerve conduits for guided peripheral nerve regeneration. *Biomaterials* 2010;31:2323–2334.
30. Schnell E, Klinkhammer K, Balzer S, Brook G, Kleeb D, Dalton P, Mey J. Guidance of glial cell migration and axonal growth on electrospun nanobers of poly-3-caprolactone and a collagen/poly-3-caprolactone blend. *Biomaterials* 2007;28:3012–3025.
31. Chew SY, Mi R, Hoke A, Leong KW. The effect of the alignment of electrospun brous scaffolds on Schwann cell maturation. *Biomaterials* 2008;29:653–661.
32. Horan RL, Antle K, Collette AL, Wang Y, Huang J, Moreau JE, Volloch V, David L, Kaplan DL, Altman GH. In vitro degradation of silk fibroin. *Biomaterials* 2005;26:3385–3393.
33. Yang Y, Chen X, Ding F, Zhang P, Liu J, Gu X. Biocompatibility evaluation of silk fibroin with peripheral nerve tissues and cells in vitro. *Biomaterials* 2007;28:1643–1652.
34. Yang YM, Zhao YH, Gu Y, Yan XL, Liu J, Ding F, Gu XS. Degradation behaviors of nerve guidance conduits made up of silk fibroin in vitro and in vivo. *Polym Degrad Stab* 2009;94:2213–2220.
35. Tang X, Xue CB, Wang YX, Ding F, Yang YM, Gu XS. Bridging peripheral nerve defects with a tissue engineered nerve graft composed of an in vitro cultured nerve equivalent and a silk fibroin-based scaffold. *Biomaterials* 2012;33:3860–3867.
36. Numat KJ, Subramanian B, Currie HA, Kaplan DL. Bioengineered silk protein-based gene delivery systems. *Biomaterials* 2009;30: 5775–5784.
37. Mandal BB, Kundu SC. Calcium alginate beads embedded in silk fibroin as 3D dual drug releasing scaffolds. *Biomaterials* 2009;30: 5170–5177.
38. Pritchard EM, Valentin T, Boison D, Kaplan DL. Incorporation of proteinase inhibitors into silk-based delivery devices for enhanced control of degradation and drug release. *Biomaterials* 2011;32: 909–918.
39. Madduri S, Papalo İzos M, Gander B. Tropically and topographically functionalized silk fibroin nerve conduits for guided peripheral nerve regeneration. *Biomaterials* 2010;31:2323–2334.
40. Wang XQ, YuceIT, Lu Q, Hu X, Kaplan DL. Silk nanospheres and microspheres from silk/pva blend films for drug delivery. *Biomaterials* 2010;31:1025–1035.
41. Uebersax L, Mattotti M, Papaliozos M, Merkle HP, Gander B, Meinel L. Silk fibroin matrices for the controlled release of nerve growth factor (NGF). *Biomaterials* 2007;28:4449–4460.
42. Herrup K, Shooter EM. Properties of the beta nerve growth factor receptor of avian dorsal root ganglia. *Proc Natl Acad Sci USA* 1973;70:3884–3888.
43. Cheng Q, Peng TZ, Hu XB, Yang CF. Charge-selective recognition at fibroin-modified electrodes for analytical application. *Anal Bioanal Chem* 2005;382:80–84.
44. Yasuda T, Sobue G, Ito T, Mitsuma T, Takahashi A. Nerve growth factor enhances neurite arborization of adult sensory neurons: A study in single-cell culture. *Brain Res* 1990;524:54–63.
45. Romero MI, Rangappa N, Li L, Lightfoot E, Garry MG, Smith GM. Extensive sprouting of sensory afferents and hyperalgesia induced by conditional expression of nerve growth factor in the adult spinal cord. *J Neurosci* 2000;20:4435–4445.
46. Gold BG. Axonal regeneration of sensory nerves is delayed by continuous intrathecal infusion of nerve growth factor. *Neuroscience* 1997;76:1153–1588.
47. Valmikinathan CM, Defroda S, Yu XJ. Polycaprolactone and bovine serum albumin based nanofibers for controlled release of nerve growth factor. *Biomacromolecules* 2009;10:1084–1089.
48. Zhang YZ, Wang X, Feng Y, Li J, Lim CT, Ramakrishna S. Coaxial electrospinning of (fluorescein isothiocyanate-conjugated bovine serum albumin)-encapsulated poly(E-caprolactone) nanofibers for sustained release. *Biomacromolecules* 2006;7:1049–1057.
49. He C, Chen Z. Enhancement of motor nerve regeneration by nerve growth factor. *Microsurgery* 1992;13:151–154.
50. Pu LLQ, Syed SA, Reid M, Patwa H, Goldstein JM, Forman DL, Thomson J.. Effects of nerve growth factor on nerve regeneration through a vein graft across a gap. *Plast Reconstr Surg* 1999;104: 1379–1385.
51. Krewson CE, Klarman ML, Saltzman WM. Distribution of nerve growth factor following direct delivery to brain interstitium. *Brain Res* 1995;680:196–205.
52. Mizuseki K, Sakamoto T, Watanabe K, Muguruma K, Ikeya M, Nishiyama A, Arakawa A, Suemori H, Nakatsuji N, Kawasaki H, Murakami F, Sasai Y. Generation of neural crest-derived peripheral neurons and floor plate cells from mouse and primate embryonic stem cells. *Proc Natl Acad Sci USA*. 2003;100:5827–5833.